Acta Chemica Scandinavica A 32 (1978) 653–657

Magnetic Structures and Properties of $Mn_{1-t}Cr_tAs$ ($0 < t \leq 0.40$)

KARI SELTE,[a] ARNE KJEKSHUS,[a] PER G. PETERZÉNS[a] and ARNE F. ANDRESEN[b]

[a] Kjemisk Institutt, Universitetet i Oslo, Blindern, Oslo 3, Norway and [b] Institutt for Atomenergi, Kjeller, Norway

$Mn_{1-t}Cr_tAs$ (MnP type structure) takes a double, helimagnetic structure with propagation vector along *a* for $\sim 0.10 \leq t \leq 0.35$ and along *c* for $0.40 \leq t \leq 1$. The spirals are conical for $0.25 \leq t \leq 0.35$. The results are discussed in relation to data for other $Mn_{1-t}T_tAs$ phases (T= V, Fe, Co, Ni). At low temperatures $Mn_{1-t}Cr_tAs$ shows a small miscibility gap ($0.01 < t < 0.10$ at 10 K).

Among the binary and ternary 3*d* transition metal mono arsenides with the MnP type structure, Mn rich $Mn_{1-t}T_tAs$ phases have recently received considerable attention due to their interesting variety of helimagnetism. For T= V, Fe, Co, and Ni the cooperative magnetic state is of the double, *a*-axis spiral type,[1-5] whereas for T=Cr a simpler antiferromagnetic arrangement has been proposed.[6] However, the brief experimental data presented in Ref. 6 are apparently also consistent with the double, *a*-axis spiral structure, and, for this reason, a reexamination of $Mn_{1-t}Cr_tAs$ has been undertaken.

EXPERIMENTAL

Samples were made from initial batches of MnAs and CrAs (preparational details, including purity of elements are given in Refs. 1 and 7) by a first heat treatment at 850 °C for one week. All samples were crushed and subjected to 2–3 further annealings for one week at 850 °C, before finally being cooled slowly to room temperature. The experimental details concerning X-ray and neutron diffraction are described in Ref. 8.

RESULTS AND DISCUSSION

(i) *Chemical crystal structure.* The room temperature unit cell dimensions of $Mn_{1-t}Cr_tAs$ are shown in Fig. 1 as functions of the composition parameter *t*. The revised phase diagram for the pseudo-binary MnAs–CrAs system on the basis of these and other findings is presented in Fig. 2.

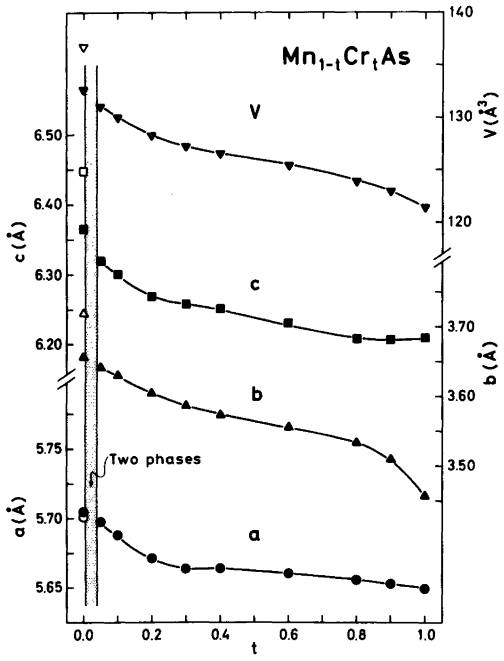

Fig. 1. Room temperature (extrapolated for MnAs) unit cell dimensions of ternary solid solution series MnAs–CrAs *versus* composition. Error limits do not exceed size of symbol. Open symbols for MnAs represent data for its NiAs type structure at room temperature.

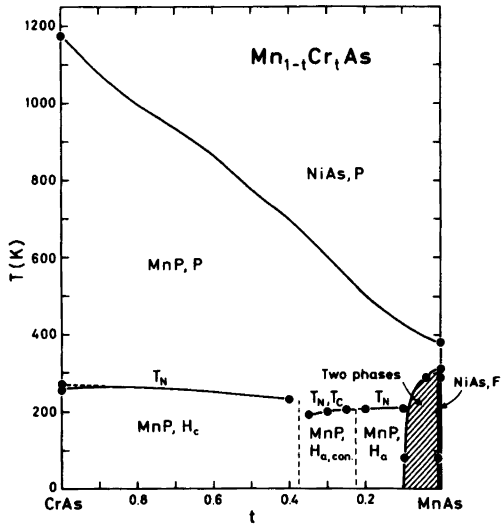

Fig. 2. Phase diagram for the pseudo-binary MnAs–CrAs system. Magnetic state is indicated by: P, para; F, ferro; H, helical.

This diagram differs *inter alia* from Kazama and Watanabe's version by the small, low temperature pocket of two phases near MnAs. The gap in the solid solubility of MnAs and CrAs is so narrow that this feature was overlooked until the structural and magnetic properties of the most Mn rich samples were compared. The present study has not been concerned with samples with (Mn+Cr)/As ratios different from 1.00.

At room temperature the MnP type atomic arrangement is stable in the interval $0.04 \leq t \leq 1$, whereas the NiAs type prevails in the immediate vicinity of MnAs. The diffraction data show that the substituted atoms are distributed randomly in the metal sub-lattice, unit cell dimensions and positional parameters for the samples studied by neutron diffraction being given in Table 1.

In common with other pseudo-binary systems of the type MnAs–*T*As,[1-5] Mn rich $Mn_{1-t}Cr_tAs$ samples take an NiAs type atomic arrangement as both low (I) and high (II) temperature form, separated by a temperature interval where the

Table 1. Unit cell dimensions and positional parameters with standard deviations for some $Mn_{1-t}Cr_tAs$ samples as derived by least squares profile refinements of neutron diffraction data. (Space group *Pnma*; positions 4(*c*); overall profile reliability factors ranging between 0.029 and 0.056.)

t	T(K)	*a* (Å)	*b* (Å)	*c* (Å)	x_T	z_T	x_X	z_X
0.05	293	5.6974(4)	3.6431(16)	6.3190(30)	0.0064(21)	0.2169(19)	0.2194(8)	0.5808(30)
0.10	6	5.5655(5)	3.4908(4)	6.1596(8)	0.0046(17)	0.2035(17)	0.1974(7)	0.5822(8)
	80	5.5681(11)	3.4966(9)	6.1671(16)	0.0056(35)	0.1996(34)	0.2009(13)	0.5786(17)
	293	5.6877(6)	3.6286(14)	6.3007(25)	0.0090(30)	0.2190(27)	0.2149(9)	0.5783(25)
0.20	8	5.5767(6)	3.4917(4)	6.1728(8)	0.0052(22)	0.2092(29)	0.1981(7)	0.5809(10)
	293	5.6701(4)	3.5985(4)	6.2795(8)	0.0050(24)	0.2119(23)	0.2119(6)	0.5825(8)
0.25	10	5.5807(15)	3.4825(10)	6.1750(18)	0.006(3)	0.213(3)	0.2001(7)	0.5795(9)
	100	5.5941(17)	3.4940(11)	6.1917(21)	0.008(3)	0.227(4)	0.1984(7)	0.5796(9)
	293	5.6668(11)	3.5870(9)	6.2657(16)	0.011(3)	0.223(4)	0.2102(7)	0.5733(10)
0.30	10	5.5954(5)	3.4844(3)	6.1903(6)	0.002(3)	0.208(3)	0.1995(5)	0.5793(7)
	80	5.5914(7)	3.4856(4)	6.1879(8)	0.012(3)	0.207(4)	0.1987(7)	0.5802(9)
	170	5.6057(6)	3.5093(3)	6.2061(7)	0.009(3)	0.205(3)	0.2029(6)	0.5784(8)
	293	5.6626(4)	3.5807(3)	6.2609(6)	0.004(3)	0.216(3)	0.2094(4)	0.5790(8)
0.35	10	5.6042(6)	3.4812(3)	6.1951(7)	0.003(5)	0.219(5)	0.2002(6)	0.5803(7)
	293	5.6642(5)	3.5783(3)	6.2562(7)	0.008(4)	0.205(4)	0.2095(5)	0.5832(8)
0.40	10	5.6359(10)	3.5925(11)	6.2082(18)	−0.006(8)	0.211(7)	0.2053(6)	0.5798(18)
	220	5.6473(10)	3.5754(5)	6.2335(5)	0.003(7)	0.217(7)	0.2065(5)	0.5812(12)
	235	5.6480(5)	3.5642(4)	6.2313(7)	0.011(6)	0.222(6)	0.2068(5)	0.5783(8)
	293	5.6599(5)	3.5694(4)	6.2464(8)	0.012(7)	0.213(6)	0.2091(5)	0.5781(8)

MnP type prevails. The second or higher order MnP⇌NiAs(II) type transition in $Mn_{1-t}Cr_tAs$ has been described by Kazama and Watanabe,[6] and we have earlier discussed the MnP⇌NiAs(I) type transition in Ref. 9.

(ii) *Magnetic structures.* As deduced from the two-phase sample of nominal composition $Mn_{0.95}Cr_{0.05}As$ (Fig. 2), the ferromagnetic mode of MnAs[10,11] extends to $t \approx 0.01$ of $Mn_{1-t}Cr_tAs$.

The double, *a*-axis type helimagnetic ordering, characteristic of $Mn_{1-t}V_tAs$ ($0.05 \leq t < \sim 0.40$),[2] $Mn_{1-t}Fe_tAs$ ($\sim 0.01 < t < \sim 0.12$),[1,4] $Mn_{1-t}Co_tAs$ ($0.05 \leq t \leq 0.15$),[3] and $Mn_{1-t}Ni_tAs$ ($0.05 \leq t < 0.07$)[5] is also found for $Mn_{1-t}Cr_tAs$ ($\sim 0.10 \leq t \leq 0.35$). For $Mn_{0.60}Cr_{0.40}As$ a double, *c*-axis type helimagnetic ordering like that of CrAs[6,7] is observed. According to Kazama and Watanabe[6] this mode covers the whole range $0.40 \leq t \leq 1$. Parameters describing these helimagnetic arrangements, are magnetic moment per metal atom (μ_T), spiral propagation vector (τ_a or τ_c), phase angle between independent spirals (ϕ_a or ϕ_c), and angle between moment and spiral axis (β), numerical values being given in Table 2 together with the Néel temperature (T_N). The two types of spiral arrangement are illustrated in Fig. 5 of Ref. 1, where also the phase relationship between the two pairs of spirals is described.

The temperature dependence of the integrated intensity of the satellites $000^{\pm}$ and $001^{\pm}$ of $Mn_{1-t}Cr_tAs$ ($0.10 \leq t \leq 0.35$) and of the satellites $000^{\pm}$, 101^{+}, 002^{-}, and 011^{-} of $Mn_{0.60}Cr_{0.40}As$ are shown in Fig. 3. From the positions and intensities of the satellite reflections, the temperature variation of μ_T, ϕ_a, and α_a (spiral turn angle) were obtained as shown in Fig. 4. Not included are curves for μ_T and ϕ_a for samples with $0.25 \leq t \leq 0.35$, due to a larger uncertainty, caused by reduced intensities of the satellites and a ferromagnetic contribution originating from a conical deformation of the spirals

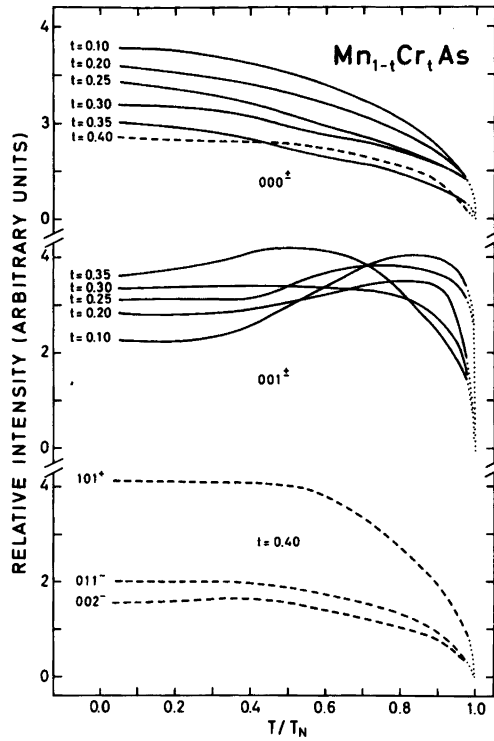

Fig. 3. Relative, integrated satellite intensities *versus* reduced temperature for $Mn_{1-t}Cr_tAs$.

(*cf.* Table 2). The appreciable variation in phase angle with temperature is characteristic for the double, *a*-axis helical mode in $Mn_{1-t}T_tAs$ (T=V, Fe, Co, Ni).[1-5] For the double, *c*-axis helical mode of $Mn_{0.60}Cr_{0.40}As$ the phase angle (Table 2) is approximately temperature independent, a feature which seems to be common for phases with this type of helimagnetic arrangement (*cf.* Refs. 5,7,8, 12–14). The turn angle increases moderately (10–15° from 0 K to T_N) independent of the

Table 2. Helimagnetic parameters for $Mn_{1-t}Cr_tAs$. Spiral propagation vector along *a* for $0.10 \leq t \leq 0.35$, along *c* for $t = 0.40$.

t	0.10		0.20	0.25	0.30	0.35	0.40
T (K)	6	80	6	10	10	10	10
$\tau_a/2\pi a^*$ or $\tau_c/2\pi c^*$	0.133(2)	0.136(2)	0.120(2)	0.097(2)	0.088(2)	0.071(3)	0.252(2)
$\mu_{T,\text{tot.}}$ (μ_B)	1.60(10)	1.60(10)	1.55(10)	1.7(1)	1.7(2)	1.6(2)	1.9(1)
ϕ_a or ϕ_c (°)	71(5)	73(5)	68(5)	60(10)	50(20)	56(20)	−122(5)
β (°)	90	90	90	62(5)	55(15)	56(15)	90
T_N (K)	210±1		208±1	205±2	202±2	195±5	232±2

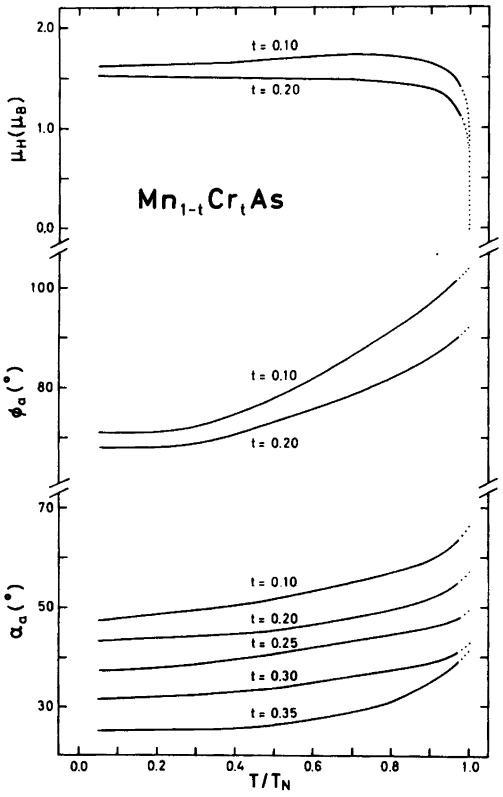

Fig. 4. Phase and turn angles and magnetic moments for *a*-axis spirals in $Mn_{1-t}Cr_tAs$ as functions of reduced temperature.

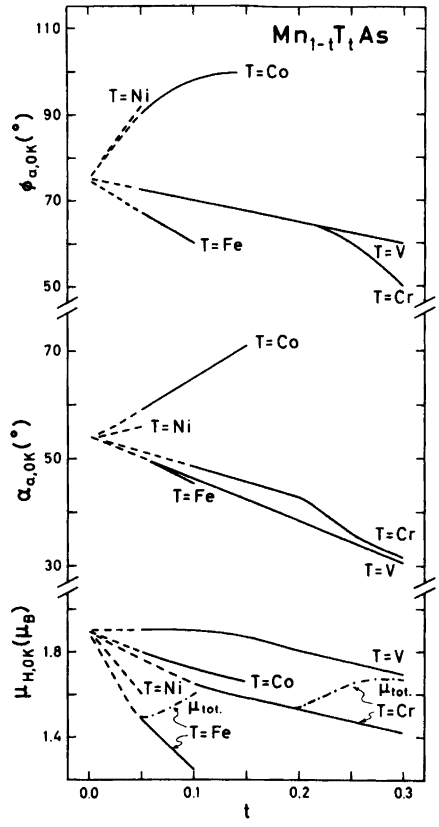

Fig. 5. Magnetic moment, turn and phase angle as functions of t in $Mn_{1-t}T_tAs$. Data refer to 0 K (extrapolated). Both helical (μ_H) and total ($\mu_{tot.}$) magnetic moments are shown for conical regions.

propagation direction of the spirals.

The variation of T_N with t (Table 2, Fig. 2) matches very closely the curves derived by Kazama and Watanabe[6] apart from the region $\sim 0.2 < t < \sim 0.5$. The designation T_N,T_C in Fig. 2 reflects the fact that the conical deformation of the double, *a*-axis helical mode (with β approximately constant) is maintained throughout the cooperative magnetic state. The consistent trend in T_N *versus* t for the different $Mn_{1-t}T_tAs$ phases is illustrated in Fig. 1 of Ref. 9. As opposed to T_N, which shows minor variation with T, the spiral parameters μ_T, α_a, and ϕ_a change markedly (Fig. 5). However, the individual characteristics extrapolate nicely to specific values for the spiral parameters of a hypothetical, helimagnetic state of MnAs ($\mu_{H,\,0\,K} = 1.9\,\mu_B$, $\alpha_{a,\,0\,K} = 54°$, $\phi_{a,\,0\,K} = 75°$, $T_N = 210$ K [9]). The implication of this on the properties of MnAs is discussed in Ref. 11.

As seen from Fig. 5, the conical deformation occurs when Mn is substituted by the nearest neighbours, Cr or Fe, in the Periodic System. The ferromagnetic component of the magnetic moment appears to be a supplement to the intrinsic helimagnetic moment. This extra contribution seems to have minor effect on the spiral parameters. However, more information is needed to explain the occurrence of the cones.

The total magnetic moment throughout the entire $Mn_{1-t}Cr_tAs$ phase shows altogether surprisingly little variation with t (between 1.6 and 1.9 μ_B). The same applies to T_N which varies between 195 and $\sim$265 K. According to considerations based on molecular field theory, this may suggest that the summed magnetic exchange interactions are approximately independent of t. On empiric basis it is commonly assumed that there is a relation between the magnetic exchange parameters and correspond-

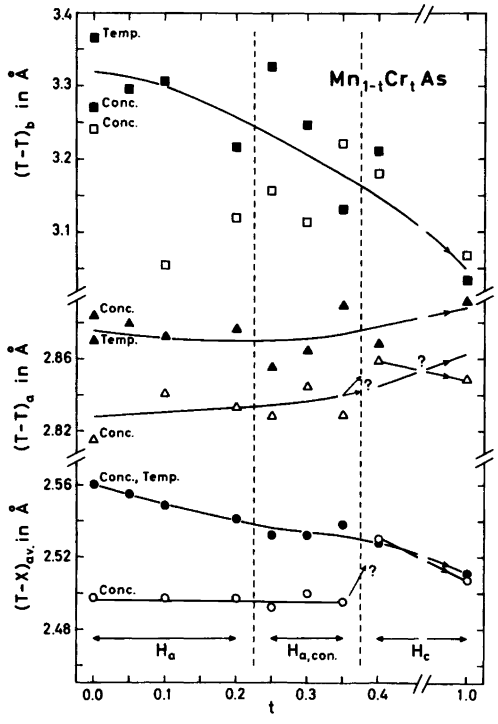

Fig. 6. Interatomic distances (average $T-X$, $T-T$ zig-zags along *a* and *b*) as functions of t in $Mn_{1-t}Cr_tAs$. Open and filled symbols refer to ~10 and 293 K, respectively. Concentration and temperature extrapolated data for MnP type MnAs are taken from Ref. 11.

ing interatomic distances. The variations with t of the shortest interatomic distances in $Mn_{1-t}Cr_tAs$ at 10 and 293 K are shown in Fig. 6. No clear-cut correlation between interatomic distances and magnetic structure is, however, evident from this illustration. In particular, the $T-T$ distance within the zig-zag chains along the *b*-axis shows large, unsystematic scattering in the experimental points.

Acknowledgement. This work has received financial support from The Norwegian Research Council for Science and the Humanities.

REFERENCES

1. Selte, K., Kjekshus, A. and Andresen, A. F. *Acta Chem. Scand. A 28* (1974) 61.
2. Selte, K., Kjekshus, A., Valde, G. and Andresen, A. F. *Acta Chem. Scand. A 30* (1976) 8.
3. Selte, K., Kjekshus, A., Valde, G. and Andresen, A. F. *Acta Chem. Scand. A 30* (1976) 468.
4. Selte, K., Kjekshus, A., Peterzéns, P. G. and Andresen, A. F. *Acta Chem. Scand. A 30* (1976) 671.
5. Delphin, I. L. A., Selte, K., Kjekshus, A. and Andresen, A. F. *Acta Chem. Scand. A 32* (1978) 179.
6. Kazama, N. and Watanabe, H. *J. Phys. Soc. Jpn. 30* (1971) 1319.
7. Selte, K., Kjekshus, A., Jamison, W. E., Andresen, A. F. and Engebretsen, J. E. *Acta Chem. Scand. 25* (1971) 1703.
8. Selte, K., Kjekshus, A. and Andresen, A. F. *Acta Chem. Scand. 26* (1972) 3101.
9. Selte, K., Kjekshus, A., Andresen, A. F. and Zięba, A. *J. Phys. Chem. Solids 38* (1977) 719.
10. Bacon, G. E. and Street, R. *Nature 175* (1955) 518.
11. Zięba, A., Selte, K., Kjekshus, A. and Andresen, A. F. *Acta Chem. Scand. A 32* (1978) 173.
12. Selte, K., Hjersing, H., Kjekshus, A. and Andresen, A. F. *Acta Chem. Scand. A 29* (1975) 312.
13. Selte, K., Hjersing, H., Kjekshus, A., Andresen, A. F. and Fischer, P. *Acta Chem. Scand. A 29* (1975) 695.
14. Selte, K., Kjekshus, A., Aaby, S. and Andresen, A. F. *Acta Chem. Scand. A 29* (1975) 810.

Received February 15, 1978.